DEPARTMENT OF COMMERCE
SINCLAIR WEEKS, Secretary

WEATHER BUREAU
F. W. REICHELDERFER, Chief

MONTHLY WEATHER REVIEW

JAMES E. CASKEY, JR., Editor

Volume 83
Number 3

MARCH 1955

Closed May 15, 1955
Issued June 15, 1955

ON THE NUMERICAL PREDICTION OF PRECIPITATION

J. SMAGORINSKY [1]

Numerical Weather Prediction Unit, U. S. Weather Bureau, Washington, D. C.

and

G. O. COLLINS [1]

Short Range Forecast Development Section, U. S. Weather Bureau, Washington, D. C.

[Manuscript received March 14, 1955]

ABSTRACT

With the three-dimensional field of velocity predicted by numerical methods it is possible to predict the moisture distribution and hence the occurrence of large-scale saturation. A three-parameter model was used to predict the 12-hour precipitation for the early stages of the storms of November 24, 1950 and November 5, 1953, neglecting cloud storage, supersaturation, a possible lack of condensation nuclei, evaporation from falling droplets, and moisture sources. Large-scale orographic influences were taken into account.

A quantitative comparison of the predicted rainfall with the correspondingly large-scale smoothed observed precipitation indicates a skill comparable to that of the predicted flow. An examination of the small-scale observed rainfall indicates that in these cases convective instability resulted in large standard deviations from the large-scale average. Numerical prediction of regions of convective instability, which is also shown, could for the time being be utilized for subjective interpretation.

CONTENTS

[1] Present affiliation: Joint Numerical Weather Prediction Unit, Federal Office Building No. 4, Suitland, Md.

341693—55——1

1. INTRODUCTION

Workers in the field of numerical prediction have concerned themselves almost exclusively with the prediction of changes in the three-dimensional mass field and hence, as a direct consequence, changes in the large-scale velocity and temperature fields. The prediction of these elements is necessary though not sufficient for the prediction of the large-scale precipitation fields. Thus one finds in the literature (e. g. [7, 10]), for the most part only qualitative comparisons between numerically predicted vertical motion fields and observed precipitation.

The prediction of precipitation is a difficult task mainly for two reasons: (i) a lack of detailed knowledge of the physics of formation of cloud particles and their precipitation; (ii) the fact that, unlike the normal situation with the other meteorological elements such as pressure,

temperature, and wind, small-scale precipitation often is of much greater magnitude than the large-scale precipitation.

Our object will be to devise a dynamical large-scale precipitation model which by the application of numerical methods will enable us to predict. In what follows we will circumvent (i) by assuming [14] (a) there are always sufficient condensation nuclei, (b) no supersaturation, (c) no supercooling, (d) no non-adiabatic processes aside from those resulting from changes of state, and (e) and (f) cloud storage and evaporation from falling droplets are both negligible compared with significant amounts of precipitation. Furthermore, we will assume no moisture source outside of the atmosphere, i. e., no evaporation from the surface of the earth. The justification, for shorter periods, lies in the fact that evaporation as a function of space is generally of much smaller amplitude and much more uniform than condensation, although in the large the two must balance.[2] It is obvious that the present laminar lower boundary condition used in numerical prediction is incapable of permitting the transport of moisture across the lower boundary. In order to take evaporation sources into account we must ultimately assume a turbulent boundary layer to make possible eddy diffusion normal to the boundary.

Difficulty (ii) will, for quantitative purposes, be ignored, but will be discussed again later. It must be pointed out that as a consequence of the large non-linear interaction, even the large-scale precipitation calculations must be in error.

2. CONDENSATION

If r is the mixing ratio, then during the condensation process $dr/dt<0$, so that the condensation rate per unit volume is $-\rho_d dr/dt$, where ρ_d is the density of the dry air. Thus the rate of precipitation reaching the ground is

$$P=\int_{p_0}^{0}\frac{1}{g\rho_w}\frac{dr}{dt}\,dp \tag{1}$$

$$\frac{dr}{dt}=\begin{cases}0, & r<r_s\\ \dfrac{dr_s}{dt}, & r=r_s\end{cases} \tag{2}$$

ρ_w being the density of liquid water (1 gm. cm.$^{-3}$), p_0 the pressure at the earth's surface, and r_s the saturation mixing ratio, a function only of p, the pressure and T, the temperature. In the absence of evaporation processes, the integral is different from zero only where $dr/dt<0$. The precipitation accumulated over a period Γ is thus given by

$$\bar{P}=\int_{t}^{t+\Gamma}P\,dt \tag{3}$$

[2] W. F. Libby has reported [9] that raindrops from hurricanes and stratiform clouds are on the average 3 weeks old.

Equation (1) may be transformed to

$$P=\frac{1}{g\rho_w}\int_D \omega\,dr, \qquad D:\begin{cases}\omega<0\\ r=r_s\end{cases} \tag{4}$$

where $\omega\equiv dp/dt$ and D is the domain of integration. A schematic typical plot of $\omega/g\rho_w$ vs r is shown in figure 1. Only the shaded area thus contributes to the integral. Hence the precipitation may be computed if r, ω, T and p, are known.

In order to predict precipitation it is thus necessary to predict the moisture field as well as the three-dimensional mass field. This may be accomplished by the requirement of continuity of r:

$$\frac{\partial r}{\partial t}\equiv\frac{dr}{dt}-\mathbf{V}\cdot\nabla r-\omega\frac{\partial r}{\partial p} \tag{5}$$

where $\mathbf{V}$ is the horizontal wind vector and the velocity components and partial derivatives are taken with respect to a coordinate system in which x is positive eastward, y is positive northward, and p is positive downward. Thus with $\mathbf{V}$, ω, and r known as functions of x, y, and p, the transport terms may be computed. To calculate dr/dt, which under our assumptions is the condensation rate, we must look to thermodynamic principles.

The mixing ratio may be defined in terms of the vapor density (or absolute humidity) ρ^* by

$$\rho^*=r\rho_d \tag{6}$$

Assuming the water vapor to behave as a perfect gas we have that

$$\rho^*=\frac{e}{R^*T},\ R^*=\frac{mR}{m^*} \tag{7}$$

where e is the vapor pressure over water or ice depending on whether T is $\geq 0°$ C. or $<0°$ C., respectively, m^* is the molecular weight of water vapor, m the molecular

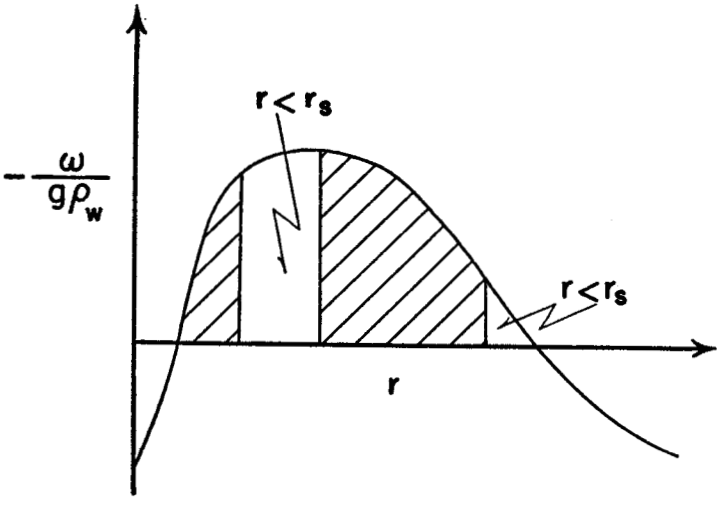

FIGURE 1.—A schematic plot of $-\omega/(g\rho_w)$ vs. r.

weight of dry air, R is the gas constant for dry air, and hence $R^*=1.608\ R$. It is assumed that the temperature of the vapor is the same as that of the dry air. Under saturated conditions $r=r_s$, and hence

$$\frac{d\ln r_s}{dt}=\frac{d\ln (e_s/T)}{dt}-\frac{d\ln \rho_d}{dt} \tag{8}$$

where e_s is the saturation vapor pressure.

The Clausius-Clapeyron equation to good approximation may be written as

$$d\ln e_s-\gamma d\ln T=0,\quad \gamma\equiv\frac{L}{AR^*T} \tag{9}$$

in which L is the latent heat of condensation and A^{-1} the mechanical equivalent of heat. For $T<0$°C. L should be replaced by the latent heat of sublimation.
Thus (8) becomes

$$\frac{d\ln r_s}{dt}=(\gamma-1)\frac{d\ln T}{dt}-\frac{d\ln \rho_d}{dt} \tag{10}$$

During the condensation process the equivalent potential temperature, θ_E, is a conservative property.

$$\frac{d\ln \theta_E}{dt}=0 \tag{11}$$

where

$$\left.\begin{aligned}&\ln\theta_E=\text{const}-\kappa\ln\rho_d+(1-\kappa)\ln T+\alpha,\\ &\alpha\equiv\frac{Lr_s}{c_pT}=\frac{\kappa m}{m^*}\gamma r_s,\\ &\kappa=\frac{AR}{c_p},\end{aligned}\right\} \tag{12}$$

and c_p is the specific heat of dry air at constant pressure. Equation (11) yields

$$\frac{d\ln T}{dt}=\frac{\alpha\dfrac{d\ln r_s}{dt}-\kappa\dfrac{d\ln\rho_d}{dt}}{\alpha-(1-\kappa)} \tag{13}$$

if the individual change of L is assumed small. Thus the individual change of temperature may be eliminated between (10) and (13) to give

$$\frac{d\ln r_s}{dt}=\Lambda\frac{d\ln\rho_d}{dt} \tag{14}$$

$$\Lambda\equiv\frac{\kappa\gamma-(1-\alpha)}{\alpha(\gamma-2)+(1-\kappa)} \tag{14a}$$

Since in these considerations the air is saturated, Λ is purely a function of p and T. Hence, as one expects, the condensation rate is proportional to the compressibility. For $p=700$ mb. and $T=0$°C.: $\alpha=.0493$ and $\gamma=19.7$. One is then justified in assuming $\alpha<<1$ and $\gamma>>2$, so that

$$\Lambda\approx\frac{\kappa\gamma-1}{\alpha\gamma+1-\kappa} \tag{15}$$

Both for small- and large-scale motions $d\rho_d/dt$ is given to good approximation by

$$\frac{d\rho_d}{dt}\approx\omega\frac{\partial\rho_d}{\partial p}$$

thus

$$\frac{d\ln r_s}{dt}\approx\Lambda\frac{\partial\ln\rho_d}{\partial p}\omega,\quad \omega<0 \tag{16}$$

Since Λ and $\partial\ln\rho_d/\partial p>0$, the side condition in (16) is required to insure that $d\ln r_s/dt<0$ for the condensation process.

Equations (1), (2), (5), and (16) taken together with a knowledge of $\mathbf{V}$ and ω suffice for the prediction of precipitation, given as initial conditions the spatial distribution of mass and mixing ratio.

With the approximation that $\omega\approx w\partial p/\partial z$, where w is the vertical velocity when the height, z, is a vertical coordinate, that $\dfrac{\partial p}{\partial z}\approx-g\rho_d$ by the hydrostatic approximation, and that the lapse rate is moist adiabatic, (16) reduces to a result deduced by Fulks [8]. Fulks did not intend to use this result prognostically but rather to calculate precipitation by means of an analogue of equation (1) from a known field of r, T, w, and p. However, we have shown equation (4) sufficient to calculate contemporary precipitation.

3. VERTICAL MOTION

The large-scale field of vertical motion is not an observable quantity. However, application of the hydrostatic and geostrophic filtering approximations to the primitive hydrodynamic equations permits one to deduce the vertical motion field given only the three-dimensional mass (or pressure) field and appropriate boundary conditions. This can be seen from the following differential equations [7]:

$$\left(\frac{\partial}{\partial t}+\mathbf{V}\cdot\nabla\right)\eta=\eta\frac{\partial\omega}{\partial p} \tag{17}$$

$$\left(\frac{\partial}{\partial t}+\mathbf{V}\cdot\nabla+\omega\frac{\partial}{\partial p}\right)\ln\theta=0 \tag{18}$$[3]

[3] There is apparent inconsistency in the use of the adiabatic approximation in the thermodynamic energy equation (18) to predict the three-dimensional velocity. By this, we assume that the heat of condensation does not materially alter the field of flow over periods of the order 24-36 hours. However, there is evidence that for longer periods, all non-adiabatic sources and sinks, orography and skin friction result in significant interactions [11]. In the present situation we may regard the approximation as a quasi-linearization with respect to the condensation in analogy with small perturbation theory where one assumes that the basic flow determines the propagation of a disturbance, but that this disturbance does not affect the mean flow to the first order of small quantities.

in which we take

$$\left.\begin{aligned} \mathbf{V}&=\frac{1}{f}\,\mathbf{k}\times\nabla\phi \\ \phi&=g\,z \\ T&=-\frac{p}{R}\frac{\partial\phi}{\partial p} \\ \eta&=\frac{1}{f}\nabla^2\phi+f \\ \ln\theta&=\text{const}+\frac{c_v}{c_p}\ln p+\ln\left(-\frac{\partial\phi}{\partial p}\right) \end{aligned}\right\} \tag{19}$$

f is the Coriolis parameter and c_v is the specific heat of air at constant volume.

In deriving the vorticity equation (17) the vertical advection of vorticity, $\omega\partial\eta/\partial p$, and the turning of the vortex tubes in vertical planes, $\frac{\partial\omega}{\partial x}\frac{\partial v}{\partial p}-\frac{\partial\omega}{\partial y}\frac{\partial u}{\partial p}$, have been neglected.

Since initially z is given as a function of x, y, and p, system (17), (18) and (19) may be regarded as two differential equations in two unknowns: $\partial z/\partial t$ and ω. Customarily ω is eliminated and the system solved for $\partial z/\partial t$. Then ω can be determined explicitly by substituting back either into (17) or (18). However, we may alternatively eliminate $\partial z/\partial t$ and write the differential equation governing ω:

$$\nabla^2\omega-\left(\frac{pf^2}{RS}\right)\frac{\partial^2\omega}{\partial p^2}=\frac{1}{S}\left(\frac{pf}{R}\frac{\partial J}{\partial p}-\nabla^2\Theta\right) \tag{20}$$

in which we abbreviated

$$\left.\begin{aligned} S&\equiv\frac{1}{T}\frac{\partial\ln\theta}{\partial p} \\ \Theta&\equiv\mathbf{V}\cdot\nabla T \\ J&\equiv-\mathbf{V}\cdot\nabla\eta \end{aligned}\right\} \tag{21}$$

For simplicity, we have replaced η by f when η occurs as a coefficient and also have assumed $\partial\theta/\partial p$, the static stability, to be constant in an isobaric surface, an approximation effectively made in all two-parameter models.

This three-dimensional Poisson equation may be solved by relaxation methods, once given the three-dimensional mass distribution which is sufficient to determine the inhomogeneous terms, and also given boundary conditions at $p=p_0$, $p=0$, and at the lateral boundaries. Consistent with a two-parameter model ω may be expressed as a quadratic function of p. Taking

$$\left.\begin{aligned} &\omega=\omega_0,\ p=p_0 \\ &\omega=0,\ \ p=0 \end{aligned}\right\} \tag{22}$$

then ω may be expressed in terms of the vertical motion, ω^*, at the level $p^*=p_0/2$:

$$\omega=[-(2\omega^*-\omega_0)\,p+(4\omega^*-\omega_0)\,p^*]\,\frac{p}{2p^{*2}} \tag{23}$$

Equation (20) may then be written as

$$\nabla^2\omega+\left[\frac{2f^2}{(2p^*-p)\,RS}\right]\omega=\frac{1}{S}\left[\frac{pf}{R}\frac{\partial J}{\partial p}-\nabla^2\Theta+\frac{pf^2}{p^*(2p^*-p)\,R}\,\omega_0\right] \tag{24}$$

We have thus reduced the problem to one of the solutions of a two-dimensional Helmholtz equation into which the boundary conditions at the top and bottom of the atmosphere already have been incorporated.

The surface vertical velocity, w_0, is induced by orography or by skin frictional action and is given by [5]

$$w_0\approx\mathbf{V}_0\cdot\nabla h+\sqrt{\frac{K}{2f}}\sin(2\nu)\,\zeta_0 \tag{25}$$

where h is the elevation of the large-scale orography, ζ_0 is the geostrophic relative vorticity in the friction layer, K is the average eddy diffusivity and ν the angle between the wind and isobars.

4. SPECIALIZATION TO A THREE-PARAMETER MODEL

For the purposes of actual calculation, the general prediction equations are reduced to a three-layered model as described in general by Charney and Phillips [7] and in particular by Charney [4]. This model is equivalent to an atmosphere consisting of three divergent barotropic layers.

The vertical velocity may be computed from the thermodynamic energy equation (18) which may be rewritten

$$w\approx\frac{1}{g}\frac{\partial\phi}{\partial p}\,\omega=\left(g\,\frac{\partial\overline{\ln\theta}}{\partial p}\right)^{-1}\frac{D}{Dt}\left(-\frac{\partial\phi}{\partial p}\right) \tag{26}$$

where D/Dt is the horizontal individual time derivative and a bar denotes the standard value. A quasi-linearization has been performed so that when the stability appeared as a coefficient, the standard atmosphere stability is used. This is consistent with the approximations made in deriving the prediction equations for this model.

The numerical integration scheme used here carries the history of the motion in the potential vorticity. Hence $\partial\phi/\partial t$ is never calculated explicitly. It is thus necessary to approximate $\partial\phi/\partial t$ in (26) by finite differences. In numerically integrating the potential vorticity equation, it is necessary to perform the initial time integration noncentrally over one finite difference time interval and thence to proceed by means of centered time differences over double time intervals [7]. The result is that a small oscillation in ϕ with a period of two time intervals is artificially induced.[4] This oscillation is barely detectable; however,

[4] This was observed by one of the writers who participated in the ENIAC calculation of the first barotropic predictions [6]. The hourly forecast data were available for inspection since the internal memory limitations of the ENIAC required the output of all intermediate results.

where time differences of the ϕ field are taken over an odd number of time intervals, a significant error is introduced. In the case of differences over one time interval, the oscillation in some instances completely masks the physically real finite difference approximation to the continuous time derivative. Therefore in the present calculations, all time differences are taken over a double interval.

In finite difference form (i and j are horizontal coordinates, k pressure, and τ time and the corresponding intervals between integral values of these coordinates are Δs, Δs, Δp, and Δt, respectively) equation (26) becomes

$$w^{\tau}_{ijk+\frac{1}{2}} = -\frac{\bar{\theta}_{k+\frac{1}{2}}}{g(\bar{\theta}_k - \bar{\theta}_{k+1})}\left(\frac{\mathfrak{D}}{\mathfrak{D}t}\right)^{\tau}_{ijk+\frac{1}{2}}(\phi_k - \phi_{k+1})^{\tau}_{ij} \tag{27}$$

where

$$\left.\begin{aligned}\left(\frac{\mathfrak{D}}{\mathfrak{D}t}\right)^{\tau}_{ijk+\frac{1}{2}}\sigma^{\tau}_{ij} &\equiv \frac{(\sigma^{\tau+1}-\sigma^{\tau-1})_{ij}}{2\Delta t} - \frac{m^2_{ij}}{4(\Delta s)^2 f_{ij}}\Im_{ij}(\sigma, \phi_{k+\frac{1}{2}})^{\tau}_{ij}\\ \Im_{ij}(a,b) &\equiv (a_{i+1}-a_{i-1})_j(b_{j+1}-b_{j-1})_i - (a_{j+1}-a_{j-1})_i(b_{i+1}-b_{i-1})_j\end{aligned}\right\} \tag{28}$$

and m_{ij} is the map scale factor. Since the ϕ field is predicted at integral values of k, we approximate $\phi_{k+\frac{1}{2}}$ by $(\phi_k + \phi_{k+1})/2$ giving

$$\left.\begin{aligned}w^{\tau}_{ijk+\frac{1}{2}} &= E_{k+\frac{1}{2}}[(\phi_{k+1}-\phi_k)^{\tau+1} - (\phi_{k+1}-\phi_k)^{\tau-1} + F\Im(\phi_k, \phi_{k+1})^{\tau}]_{ij}\\ E_{k+\frac{1}{2}} &\equiv \frac{\bar{\theta}_{k+\frac{1}{2}}}{2\Delta t g(\bar{\theta}_k - \bar{\theta}_{k+1})}\\ F_{ij} &\equiv \frac{\Delta t}{2(\Delta s)^2}\left(\frac{m^2}{f}\right)_{ij}\end{aligned}\right\} \tag{29}$$

$\Delta s = 300$ km., $\Delta t = \frac{1}{2}$ hr., and m_{ij}^2 is taken to be unity for the latitude span used here on a Lambert conformal projection (see for example [12]), $k = 1, 1\frac{1}{2}, 2, 2\frac{1}{2}, 3$ refer to 200, 350, 500, 675, 850 mb., respectively, and the boundaries $k = \frac{1}{2}$, $k = 3\frac{1}{2}$ are placed at 25 mb. and 1000 mb., respectively.

w can first be computed centrally over a double time interval at $t = \frac{1}{2}$ hour using information at $t = 0$, and $t = 1$ hour. The initial vertical velocities at $t = 0$ are therefore taken to be the same as those at time $t = \frac{1}{2}$ hour. Inspection of the subsequent data showed that changes within a half hour interval are sufficiently small that no serious error is introduced by this assumption.

Since the vertical velocities computed by the model, especially those at 350 mb., are at rather high levels in the troposphere and above the maximum concentration of moisture, it is considered necessary, for the prediction of precipitation, to deduce vertical velocities at lower levels. Predictions with models giving greater definition at lower levels, e. g., a three-layer model with p^2 the vertical coordinate [4] which gives values at about 575 and 825 mb. or perhaps a five-level model, may eliminate this need to interpolate. Given w at four levels: 675, 350 mb. and the boundaries 1000 and 25 mb., one can fit a cubic with respect to pressure, giving a continuous function:

$$^1w(p) = M(p)w_{675} + N(p)w_{350} \tag{30}$$

in which M and N are the interpolation variables, and the anterior superscript denotes first approximation.

As previously pointed out, the computations of vertical velocities in this particular model are based on the assumption that the vertical velocity is zero at 1000 mb., the lower boundary. This assumption may not produce serious errors in the prediction of the geopotential field but does become more detrimental in the prediction of precipitation. Vertical velocities at the surface produced by forced ascent over orographic barriers can contribute considerably to the precipitation [10]. The most logical and consistent way to include the effects of large-scale varying terrain would be to incorporate this lower boundary condition implicitly in the prediction equations. This can be done without great difficulty (see for example eq. (24)). Since the flow prediction equations used here do not take terrain into account, these effects are included a posteriori. Vertical velocities at the lower boundary, 1000 mb., are computed from (see eq. (25))

$$w_0 = \mathbf{V}_0 \cdot \nabla h \approx \mathbf{V}_{900} \cdot \nabla h \tag{31}$$

where $\mathbf{V}_{900}$ is the geostrophic wind at 900 mb. $\mathbf{V}_{900}$ was extrapolated quadratically from information at 200, 500, and 850 mb. For a second approximation to the vertical velocity we define

$$^2w(p) = {}^1w(p) + \frac{p}{1000}w_0 \tag{32}$$

While this procedure is somewhat arbitrary, it has the characteristic, somewhat similar to that of the atmosphere, that the effects of the lower boundary on the flow are damped out approximately linearly with decreasing pressure. Vertical velocities may be calculated in this manner for $p = 400(100)900$mb. denoted by $k' = 1$ to 6, respectively.

In the integration of the finite difference form of the potential vorticity equation the choice of Δt was bounded by the requirement of computational stability with respect to Δs. Since there is no such restriction in using the results of the integration of the potential vorticity equation together with the finite difference form of the system (1), (2), (5), and (16), a time interval, $\Delta' t$, in precipitation equations, may be chosen commensurate only with the time scale of the dependent variables.

The ϕ field at the levels k', may be quadratically interpolated and extrapolated from the values at $k = 1, 2, 3$.

The temperature $\left(T = -\frac{p}{R}\frac{\partial\phi}{\partial p}\right)$ is predicted only at $k = 1\frac{1}{2}$ and $2\frac{1}{2}$. While a linear interpolation for intermediate levels may adequately determine the tempera-

ture, experiments in extrapolating to flanking levels prove inadequate for our purposes. This can be overcome to some extent by making selective use of the observed detail in the initial soundings. The observed initial temperatures at each level k' are smoothed subjectively yielding $T^0{}_{ijk'}$. The predicted temperature change, ΔT, at $k=1\frac{1}{2}, 2\frac{1}{2}$ over the time interval $\Delta' t$ is then interpolated and extrapolated linearly to give the temperature change at the levels k'. This process may be iterated:

$$\left.\begin{aligned} T^{\tau'+1}_{ijk'} &= [T^{\tau'}+(\Delta T)^{\tau'+\frac{1}{2}}]_{ijk'} \\ (\Delta T)^{\tau'+\frac{1}{2}}_{ijk'} &= [a_{k'}(\Delta T)_{1\frac{1}{2}}+b_{k'}(\Delta T)_{2\frac{1}{2}}]^{\tau'+\frac{1}{2}}_{ij} \end{aligned}\right\} \tag{33}$$

where $a_{k'}$ and $b_{k'}$ are determined from the interpolation formula. Since $\phi_{k'}$ is determined independently by a much simpler scheme, there will be some hydrostatic inconsistency with the corresponding $T_{k'}$ field. This may be avoided by determining $T_{k'}$ as described, but integrating vertically to obtain $\phi_{k'}$, using as a reference one of the $\phi_{k'}$'s.

The system of prediction equations (1), (2), (3), (5) and (16) in finite difference form is thus:

$$P^{\tau'}_{ij}=\frac{1}{g\rho_w}\sum_{k'}\left(\frac{dr}{dt}\right)^{\tau'}_{ijk'}(p_{k'+\frac{1}{2}}-p_{k'-\frac{1}{2}}) \tag{34}$$

$$\frac{dr}{dt}=\begin{cases}0, & r<r_s\\ \dfrac{dr_s}{dt}, & r=r_s\end{cases} \tag{35}$$

$$\bar{P}_{ij}=\sum_{\tau'}P^{\tau'}_{ij}\Delta' t \tag{36}$$

$$\left.\begin{aligned} r^{\tau'+1}_{ijk'} &= r^{\tau'-1}_{ijk'}+\delta\Delta' t\left[\left(\frac{dr}{dt}\right)_{k'}+\frac{m^2}{4(\Delta s)^2 f}\right. \\ &\left.\Im_{k'}(r,\phi)_{k'}-\omega_{k'}\left(\frac{r_{k'+1}-r_{k'-1}}{p_{k'+1}-p_{k'-1}}\right)\right]^{\tau'}_{ij} \\ \delta &= \begin{cases}1 \text{ and } r^{\tau'-1}=r^0 \text{ for } \tau'=0\\ 2 \qquad\qquad\quad \text{for } \tau'>0\end{cases} \end{aligned}\right\} \tag{37}$$

$$\left(\frac{dr_s}{dt}\right)^{\tau'}_{ijk'}=\left[r_s\Lambda\frac{(\partial \ln \rho_d)}{\partial p}\omega\right]^{\tau'}_{ijk'},\ \omega<0 \tag{38}$$

For computational convenience the density lapse rate is taken to correspond to that of the moist-adiabatic lapse rate, and hence is a function of height only. This approximation is not necessary with numerical prediction models of three or more parameters. In the present three-parameter model the static stability, although constant in the vertical, may vary in time and in the horizontal. Hence the continuous form

$$\frac{d\ln\rho_d}{dt}\approx-\omega\left(\frac{\partial\phi}{\partial p}\right)^{-1}\left(\frac{\partial^2\phi}{\partial p^2}\right)$$

in finite differences becomes

$$\left(\frac{d\ln\rho_d}{dt}\right)^{\tau}_{ijk}=\left[\frac{2\omega_k}{p_{k+1}-p_{k-1}}\left(\frac{\phi_1+\phi_3-2\phi_2}{\phi_{k+1}-\phi_{k-1}}\right)\right]^{\tau}_{ij} \tag{39}$$

At the upper and lower boundaries $\partial\phi/\partial p$ must be determined non-centrally. In all calculations, for convenience, L is taken as the latent heat of condensation, and e and r are taken with respect to water, irrespective of T. This restriction may easily be removed.

Comparisons of predicted geopotential tendencies with observed 12-hour changes [2] indicate that a time interval, $\Delta' t$, of 12 hours represents an upper limit. However, appreciable error can be introduced by the assumption that the saturation state is constant over so long an interval. It is estimated that $\Delta' t=3$ hours would result in more tolerable truncation errors. It is possible, however, to use a larger $\Delta' t$ if the truncation error resulting from the constant saturation state approximation is to some extent eliminated. This may be accomplished by estimating the time, t_s, of occurrence of change of saturation state during $\Delta' t$. One can determine from the initial mixing ratio, r^0, the saturation state at that time. In the instance where $r^0<r^0_s$, then one may determine whether saturation will occur during $\Delta' t$ from the non-central form of (37) between $t=0$ and t_s:

$$t_s=\frac{(r^0_s-r^0)_{k'}}{\left[\dfrac{m^2}{4(\Delta s)^2 f}\Im_{k'}(r,\phi)_{k'}-\omega_{k'}\left(\dfrac{r_{k'+1}-r_{k'-1}}{p_{k'+1}-p_{k'-1}}\right)\right]^0_{ij}} \tag{40}$$

t_s is thus defined and determinable. If $t_s>\Delta' t$ then $dr/dt=0$ over the entire interval. If not, dr_s/dt computed from (38) is to be weighted by the factor $(1-t_s/\Delta' t)$. For initially saturated conditions one uses a correspondingly derived criterion for the occurrence of unsaturated conditions during $\Delta' t$. Thompson and Collins [14] used a similar technique for precipitation calculations in which $\Delta' t$ was taken as 12 hours. They did not take horizontal moisture transport into account.

5. THE EXPERIMENT

The situations chosen were the early synoptically unspectacular stages of two cases of rapid cyclogenesis. The initial conditions were taken at 0300 GMT, November 24, 1950, and 1500 GMT, November 5, 1953. The object was to predict the accumulated precipitation over a 12-hour period. For this purpose $\Delta' t$ was first taken as 12 hours. With the scheme outlined in the previous section, the only predictive element is a determination of the time of occurrence of change of saturation state. Otherwise, only the initial ω and r fields are needed. A second calculation was prepared in which $\Delta' t$ was taken as 3 hours and, therefore, the full set of prediction equations were used in 4 iterations for a 12-hour forecast.

Numerical flow forecasts for the same two periods

treated here were performed by the Princeton group using a three-parameter 900–700–400-mb. model [4], but 3-hourly vertical motion fields were not calculated. The fact that these situations were highly baroclinic in the lowest levels meant that the 850–500–200-mb. model was incapable of recognizing the large amount of potential energy available for conversion to kinetic energy. The result is that the predicted development by the 850–500–200-mb. model was inferior to that by the 900–700–400-mb. model in both cases. This is particularly true for the November 5, 1953, case.

6. DISCUSSION OF RESULTS

For the purposes of verifying the forecasts of large-scale precipitation accumulating over 12-hour periods, observations from all hourly precipitation reporting stations were utilized. This of course gives a relatively fine-grained picture of the actual precipitation—with stations having an average separation of roughly 30 miles. The observations were taken from *Climatological Data for the United States* [15] and from specially prepared listings supplied by the National Weather Records Center in Asheville, N. C.

NOVEMBER 24, 1950

A comparison of the 850-mb. maps at initial time 0300 GMT (fig. 2A) and 12 hours later (fig. 2E) shows that the depression centered south of Lake Superior filled but a secondary trough was forming to the south. This is predicted by the model used (fig. 2E). At 500 mb. the Low centered in Wisconsin (fig. 2B) elongated and moved to southern Lake Michigan (fig. 2F). Again this evolution was adequately predicted (fig. 2F). At 200 mb. the flow forecast was not quite as good, but has less bearing on the present problem and is not shown. The calculated vertical motion fields at the beginning and end of this 12-hour period at 675 mb. and at 350 mb. are shown in figure 2 (C, D, G, and H). The predicted fields of ϕ and w at the intermediate 3-hourly intervals are not shown.

In figure 3A are plotted all non-zero and non-missing 12-hourly precipitation reports to the south and east of the heavy boundary. The results using $\Delta' t=12$ hours (dashed lines) indicate a maximum of .23 inch at Lake Erie. However for $\Delta' t=3$ hours (solid lines) there occurs a double maximum, one at Lake Erie of the same magnitude and another in Tennessee with somewhat larger maximum value. A comparison of non-zero points and predicted precipitation greater than .01 inch indicates a good qualitative forecast for either model and thus a fairly reliable statement of the time of onset and cessation of precipitation. However examination of the individual reports indicates large deviations even from the results using $\Delta' t=3$ hours. Figure 3B summarizes the large-scale average observed precipitation and the standard deviation from this average. This was constructed by averaging all observations within the isohyetal channels of the prediction in which $\Delta' t=3$ hours. These points were computed from over 1,300 observation stations in eastern United States. The model is seen to have over-predicted the large-scale precipitation by a factor of approximately 2 for the intermediate amounts and by a factor of 1.25 for the maximum.

It is also important to bear in mind that the three-parameter model used here (850–500–200-mb.) gives a flow forecast inferior to that of the 900–700–400-mb. model even in the first 12 hours.

It is evident from a comparison of figure 2 (C, D, G, and H) with figure 3A that upward vertical motion is only a necessary though not a sufficient condition for precipitation even for qualitative purposes. For instance one would not have judged from the vertical velocity field alone that the primary precipitation maximum would be in Tennessee.

NOVEMBER 5, 1953

This case deals with a nascent cyclone in the northeast Gulf of Mexico at 850 mb. (fig. 4A) which deepened and traveled up off the east coast to 31° N. latitude in a 12-hour period (fig. 4E). Actually the 850–500–200-mb. model gave a forecast which was quite poor in describing the observed development. No deepening and only slight eastward motion were predicted at 850 mb. (fig. 4E).

At 500 mb. the primary trough in northeastern United States (fig. 4B and F) was predicted to move too rapidly to the east and the development of a closed circulation was missed entirely. On the other hand the secondary in the Gulf, associated with the 850-mb. closed Low, was predicted to move to the east at the approximate speed observed.

It should be noted that the anticyclogenesis predicted in north-central United States at 850 mb. and 500 mb. but not observed does not directly affect the area of our precipitation forecasts.

In figure 5A we have, as before, the raw precipitation observations superimposed on forecasts computed using $\Delta' t=12$ and 3 hours.

An essential difference in the observed precipitation between this case and that of November 1950 is the occurrence of large amounts along the Carolina and southern Virginia coasts. The observed 850-mb. flow at the beginning and end of this period shows onshore winds. This coastal effect is well known [1] but is not taken into account by the present theory. Presumably this could be accomplished by an extension of the theory resulting in equation (25) to apply to variable surface roughness.

A significant difference is observed between the predictions using $\Delta' t=12$ hours and 3 hours. For $\Delta' t=12$ hours the maximum is only half as large as that for $\Delta' t=3$

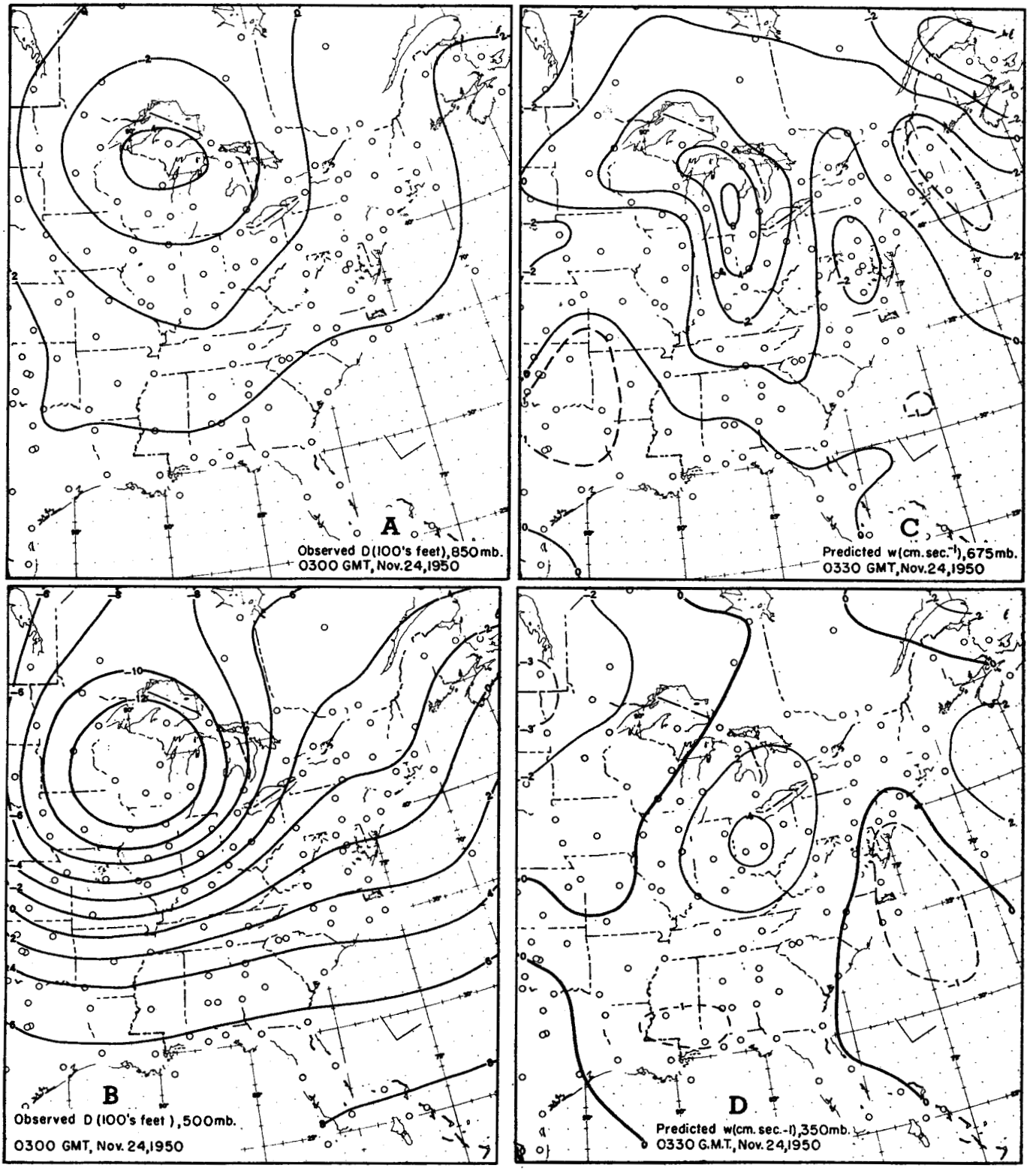

FIGURE 2.—November 24, 1950 case: initial, predicted, and verifying horizontal flow (A, B, E, F,); initial and predicted vertical flow (C, D, G, H) for the 12-hour period 0300–1500 GMT, November 24, 1950.

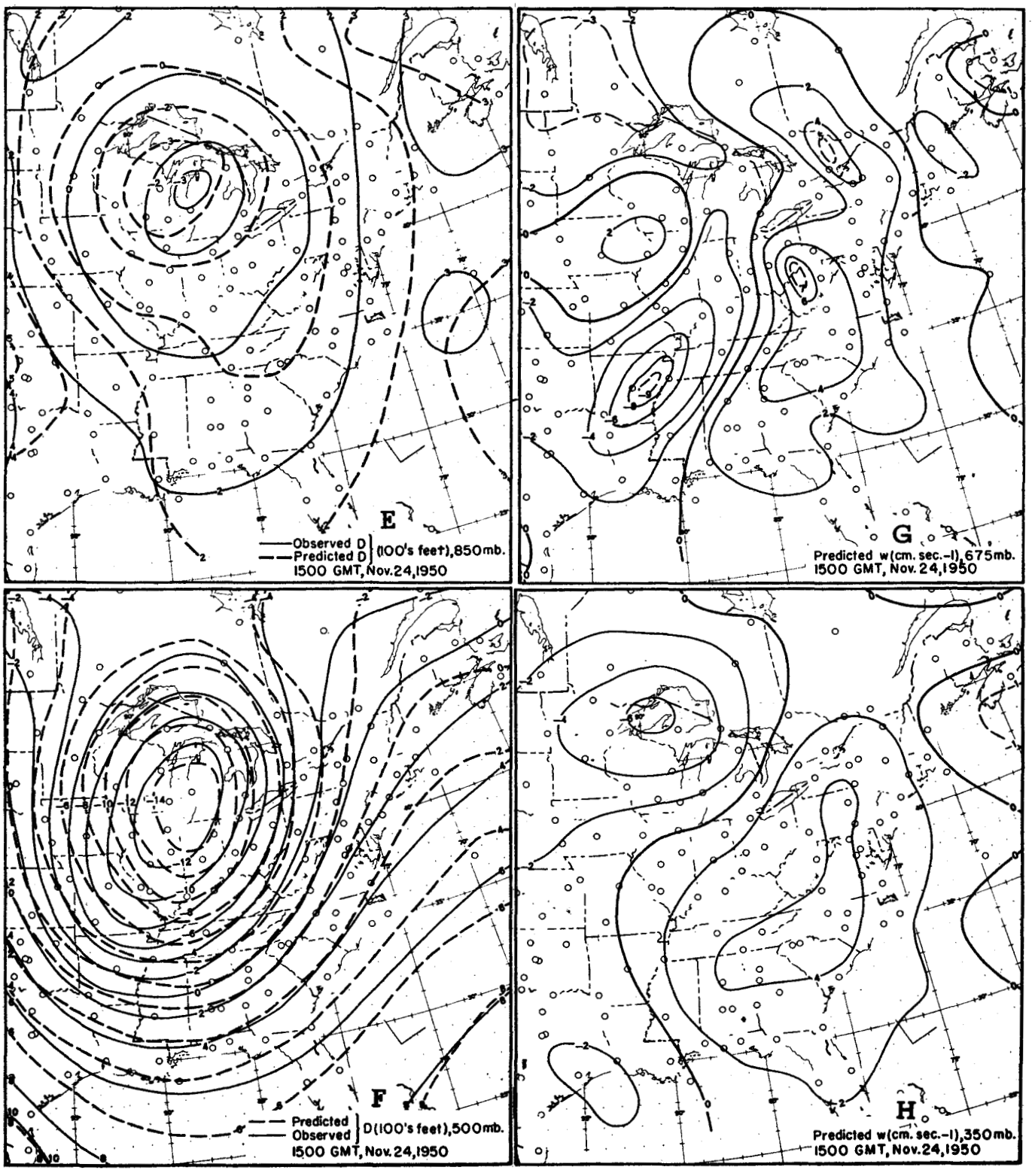

Figure 2—Continued

341693—55——2

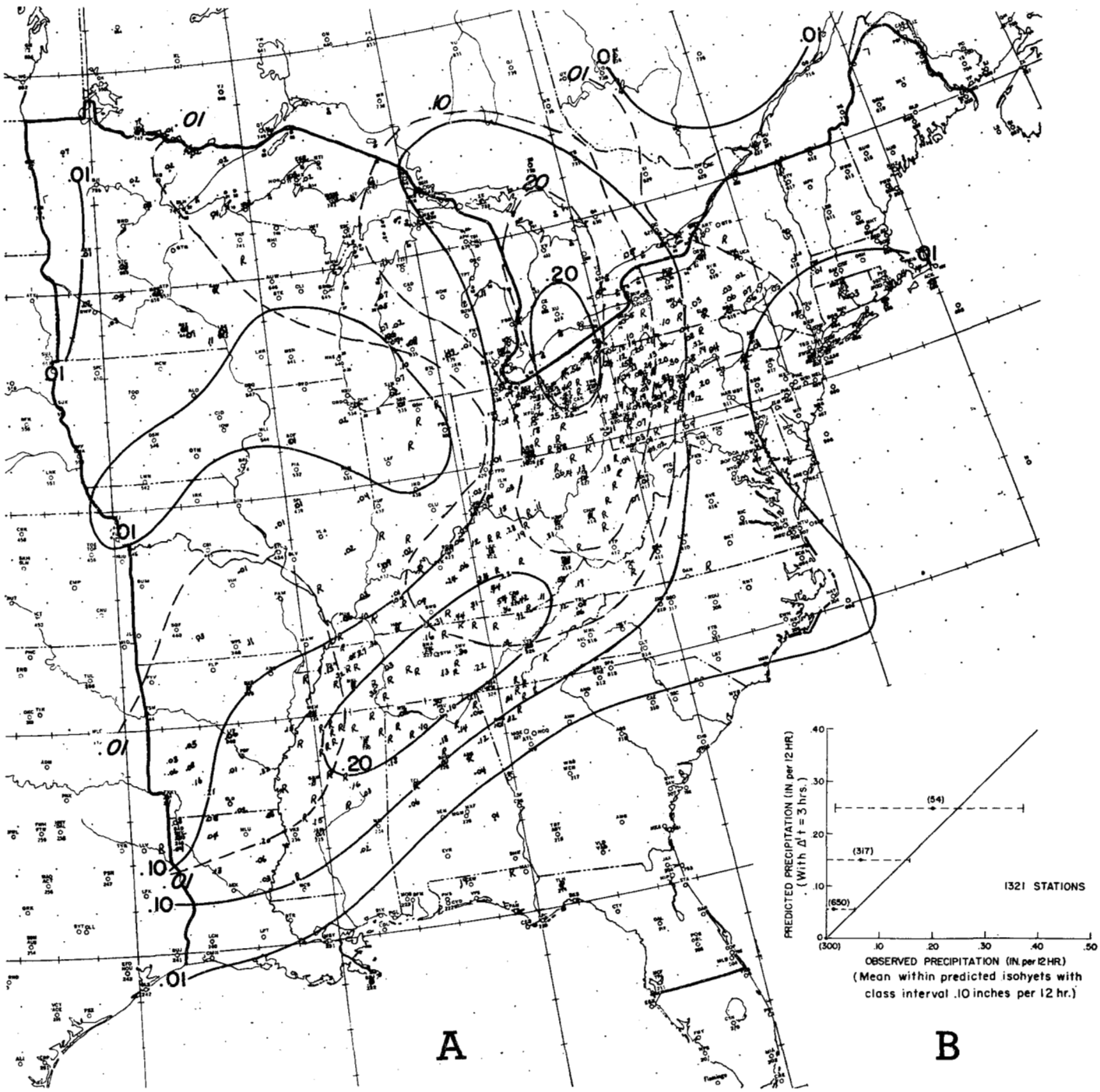

FIGURE 3.—(A) Observed precipitation during period 0300–1500 GMT November 24, 1950 with computed isohyets ($\Delta' t = 3$ hr., solid and $\Delta' t = 12$ hr., dashed) superimposed. R denotes precipitation ≥ 0.01 in. but amount is unknown and thus R is not included in the numerical verification. Missing reports and zero precipitation are not shown. (B) Summary of results with observations smoothed for large-scale verification. Numbers in parentheses at plotted points give number of stations averaged in the respective isohyetal channel. Dashed lines indicate standard deviation of observations in the respective channel.

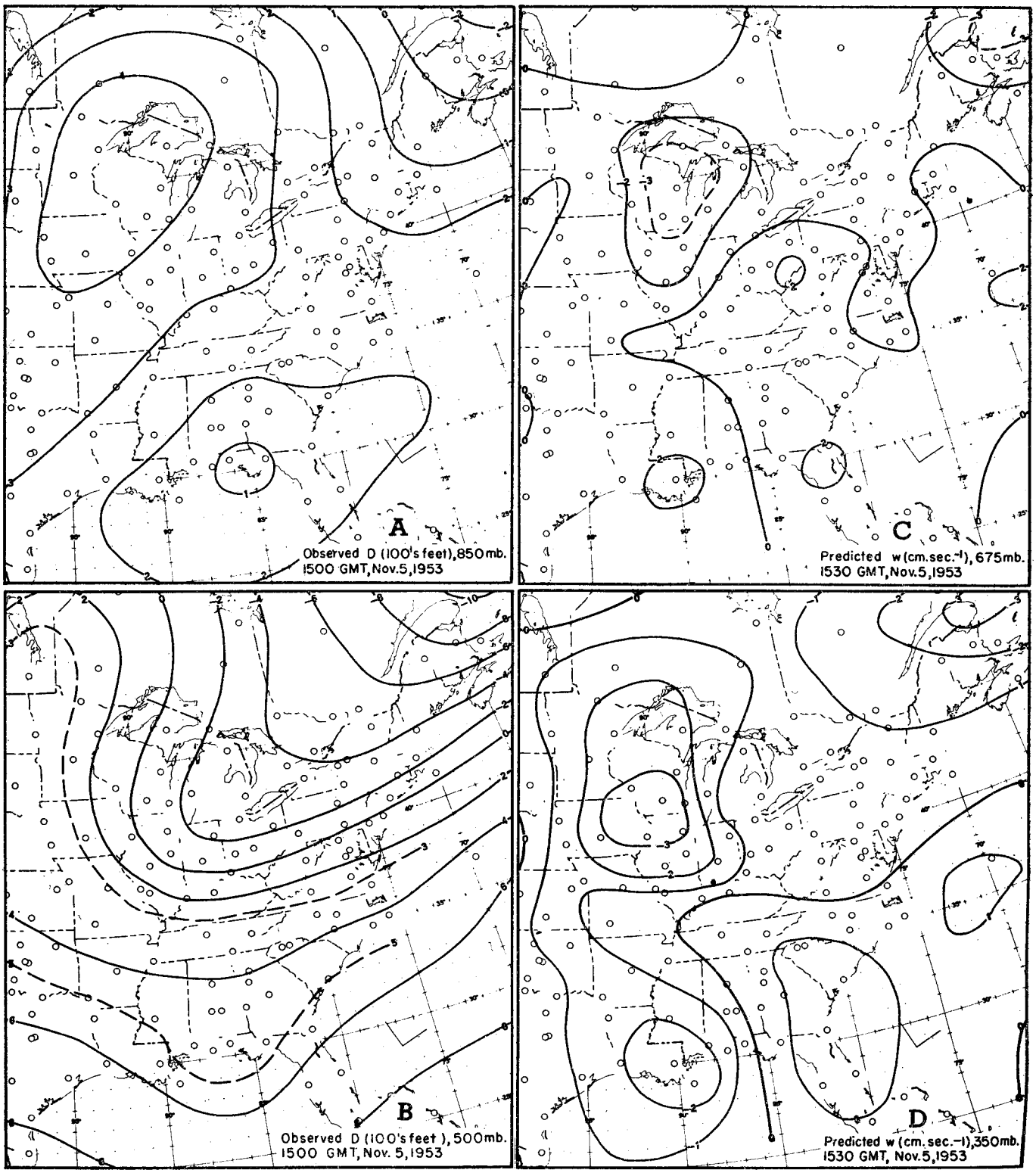

FIGURE 4.—November 5, 1953 case: initial, predicted, and verifying horizontal flow (A, B, E, F); initial and predicted vertical flow (C D, G, H) for the 12-hour period 1500 GMT November 5 to 0300 GMT November 6, 1953. See p. 64 for parts E, F, G, H.

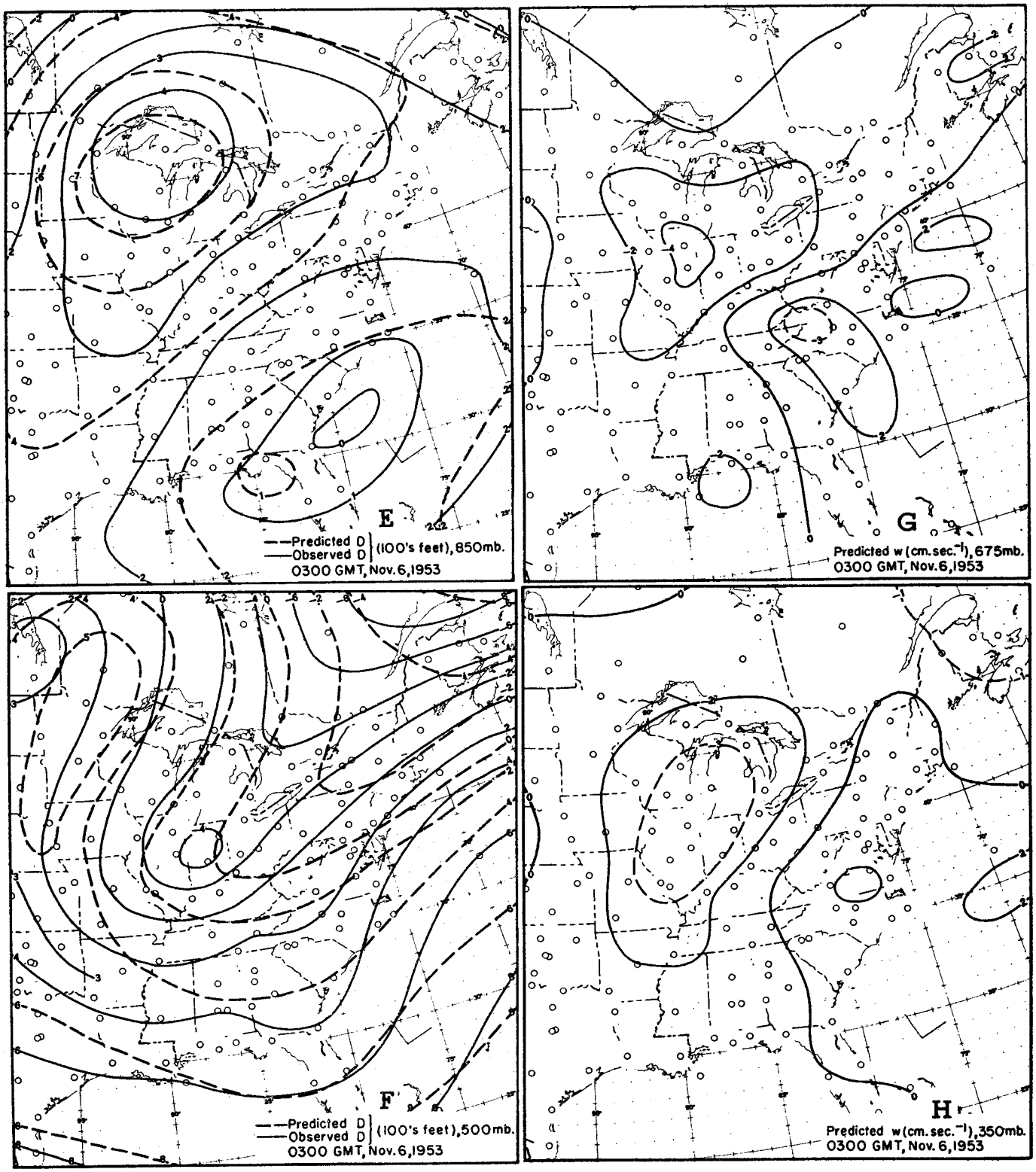

FIGURE 4.—(Continued) November 5, 1953 case: initial, predicted, and verifying horizontal flow (A, B, E, F); initial and predicted vertical flow (C, D, G, H) for the 12-hour period 1500 GMT November 5, 1953 to 0300 GMT November 6, 1953. See p. 63 for parts A, B, C, D.

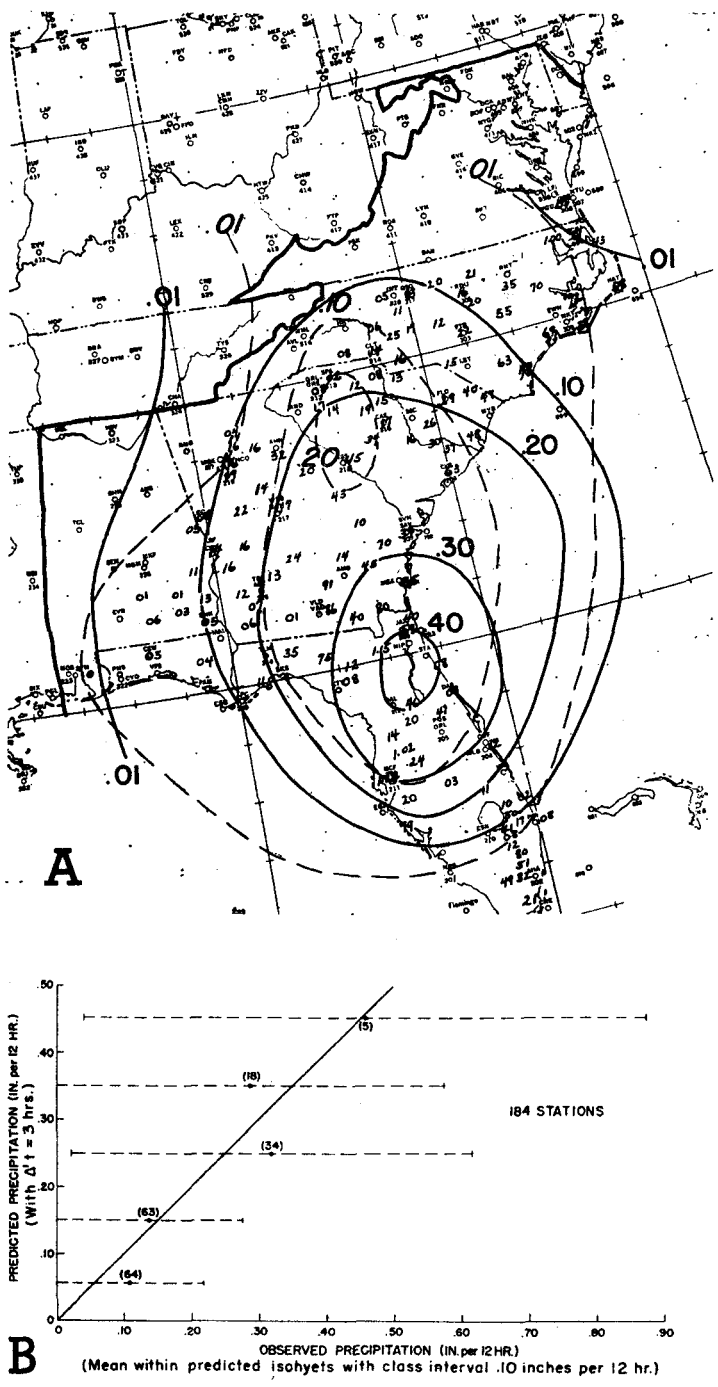

FIGURE 5.—(A) Observed precipitation during period 1500 GMT November 5 to 0300 GMT November 6, 1953 with computed isohyets ($\Delta' t = 3$ hr., solid and $\Delta' t = 12$ hr., dashed) superimposed. R denotes precipitation ≥ 0.01 in. but amount unknown and thus R is not included in the numerical verification. Missing reports and zero precipitation are not shown. (B) Summary of results with observations smoothed for large-scale verification. Numbers in parentheses at plotted points give number of stations averaged in the respective isohyetal channel. Dashed lines indicate standard deviation of observations in respective channel.

hours and is also displaced to the north. Had the flow prediction for this period been correct, as essentially resulted from the 900–700–400-mb. model, the maximum would have been elongated northeastward along the coast. However one can speculate that, in spite of this elongation, the maximum would not have been reduced because of the larger vertical velocities associated with the increased development.

In this particular case the vertical motion fields (fig. 4C, D, G, and H) would have given a fairly realistic qualitative indication of the region of precipitation without referring to the moisture field and its changes. On the other hand, the magnitude of the vertical velocity would have been misleading. In the November 24, 1950 case at 675 mb. an average maximum vertical velocity of +6.5 cm sec^{-1} yielded a predicted maximum precipitation of .23 in./12 hr., while in the November 5, 1953 case an average maximum vertical velocity of +2.5 cm sec^{-1} gave .43 in./12 hr.

In figure 5B we have a comparison of the large-scale smoothed observed precipitation vs. the computed. In this case the plotted points, representing a total of 184 observations within the verification area chosen have more-or-less uniform scatter about the perfect forecast line.

It is interesting to observe the occurrence of much larger standard deviations than were found in the first case. This is a normal characteristic of precipitation at lower latitudes where the incidence of convective instability is greater.

7. PREDICTION OF RELATED ELEMENTS

Charts of the predicted and observed 12-hour changes in dew point at 900 mb. were prepared for the November 5, 1953 case (fig. 6). Cursory qualitative examination of the field distributions reveals an excellent correspondence. The 7.5° C. rise in western Kentucky is predicted quite well. Although the fall area in the Great Lakes region is correct, the minimum is predicted to be too far east. However, although the secondary minimum in western Virginia is correctly placed, the predicted minimum is too small in magnitude. A large discrepancy is noted over Arkansas where the observed rise is predicted as a substantial fall. On the other hand the negative band through the Gulf States, Oklahoma, Kansas is correct, although the observed minimum in the Gulf States is predicted farther to the northwest and twice too large. The rise off the southeast Atlantic Coast is correct but one-third the observed magnitude. Fortunately the discrepancies pointed out above do not greatly affect the precipitation calculations.

The details of the moisture prediction calculations show

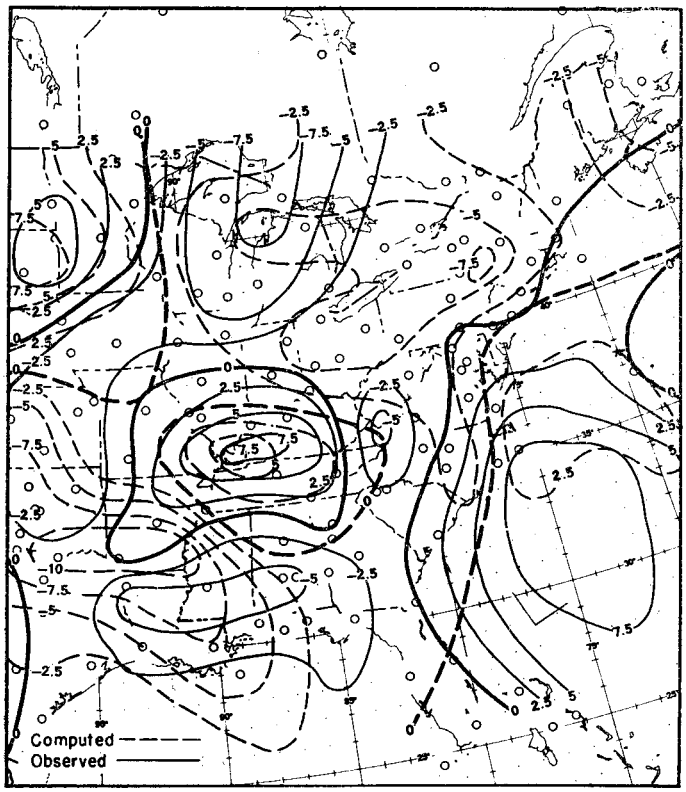

FIGURE 6.—Predicted and observed 12-hour change of dew point (°C.) at 900 mb. between 1500 GMT, November 5 and 0300 GMT, November 6, 1953.

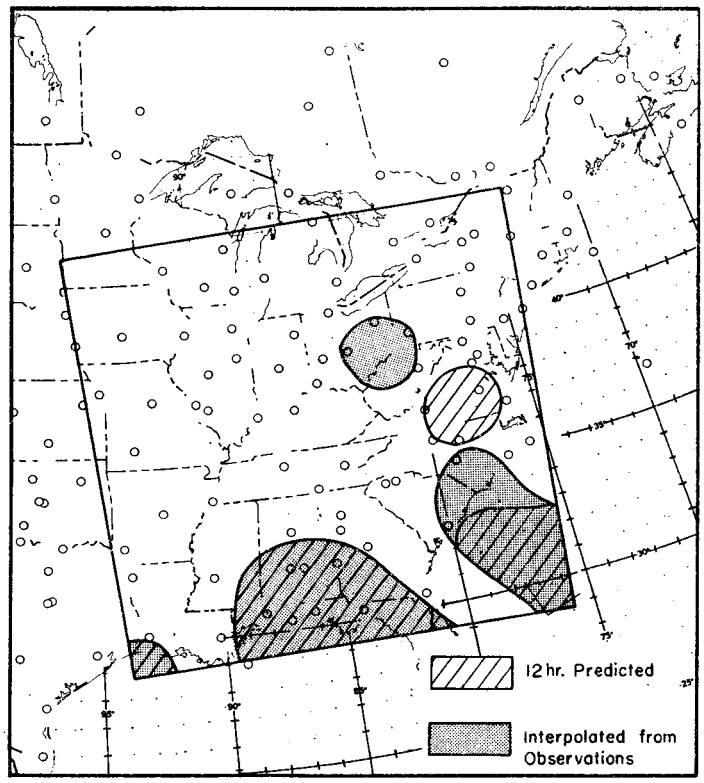

FIGURE 7.—Predicted and observed areas of convective instability ($\partial\theta_E/\partial p>0$), 0300 GMT, November 6, 1953.

that on the average, the condensation, the local time derivative of mixing ratio, and the horizontal and vertical transports of mixing ratio are all of the same magnitude. Hence any approximation neglecting one of these would be invalid.

We see that the large-scale average precipitation is on the whole predicted correctly. Thus one could expect to be able quantitatively to predict total precipitation over large watersheds the scale of a unit mesh area—approximately 35,000 sq mi. The fine structure due to small-scale instability is not capable of being predicted by the models used. For a wholly dynamical prediction, small-scale non-linear theory of the type utilized by Tepper [13] would be required. The obvious difficulty is that an extremely fine network of surface and aerological observations would be required in order to adequately specify initial conditions. For the time being this is not economically feasible operationally, even if the theory were adequately developed. For most purposes it might be sufficient if statistical moments of precipitation higher than the mean (such as the standard deviation) were somehow attainable by dynamical methods.

Thus, what suggests itself, is a statistical-mechanical approach such as is used in other branches of physical science. The fine structure itself is not predicted but rather the distribution of the statistical properties of the fine structure. Even for this modest requirement, it is necessary to understand the mechanism of convective processes in a moist atmosphere and the dependence of the small-scale dynamics on the ambient large-scale conditions.

From parcel stability considerations we have the well known result that a necessary condition for convective instability is that the equivalent potential temperature decrease with height.[5] Figure 7 shows a 12-hour forecast from the 1500 GMT, November 5, 1953 situation of the occurrence of convective instability according to the parcel criterion. It is seen that the verification with the observed occurrence is quite good, especially since the flow prediction at this time was already beginning to degenerate. The release of this instability could be accomplished, theoretically, by sufficient lifting.

8. FRICTIONAL VERTICAL VELOCITY

Although the influence of frictional divergence is not included in the prediction model, it is of interest to study the magnitude of the vertical velocity so produced in one of the cases treated. Figure 8 shows the frictional vertical

[5] Parcel dynamics have often been viewed critically, and with good reason. The most recent is an article by C. H. B. Priestley, "Buoyant Motions and the Open Parcel", *The Meteorological Magazine*, vol. 83, No. 982, April 1954, pp. 107-114.

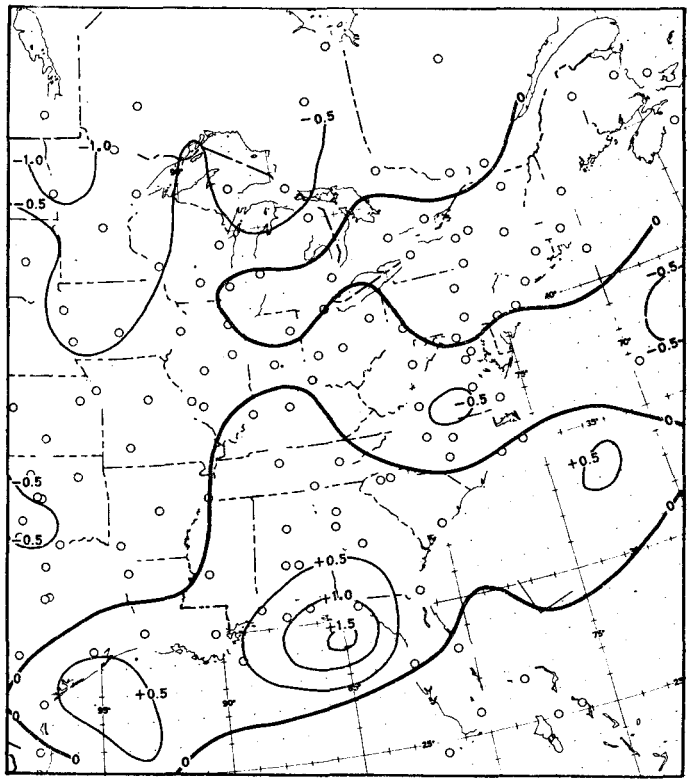

FIGURE 8.—Frictional vertical velocity (cm. sec. $^{-1}$) at top of friction layer computed at 1500 GMT, November 5, 1953.

velocity at the top of the friction layer computed from the second term of equation (25) using the observed 850-mb. flow at 1500 GMT November 5, 1953. The constants are chosen according to average values suggested by Brunt [3]:

$$K \approx 10 \text{ m.}^2 \text{ sec.}^{-1} \text{ and } \nu \approx 22.5°.$$

We see that the magnitude of the forced frictional vertical velocity can attain values of over 1 cm. sec.$^{-1}$. Assuming that this boundary influence decreases linearly with decreasing pressure (as was done for the orographic influence), the computed free vertical velocities even at 675 mb. would change by not more than 25 percent. However there may result significant shifts in the location of centers of maximum or minimum. For example the frictional maximum of +1.5 cm. sec.$^{-1}$ south of Tallahassee would result in shifting the free maximum at 675 mb. to the west over the northern Florida peninsula with little change in magnitude.

On the other hand, fields of free vertical velocity not associated with large-scale storms, and which are thus more of the magnitude of frictional vertical velocities, could undergo large percental changes, conceivably changing sign. Under proper moisture conditions this could make the difference as to whether or not small amounts of precipitation would result over large areas.

9. CONCLUDING REMARKS

The foregoing represents a rudimentary physical framework by which the occurrence of precipitation may be predicted. The reality of the results may be thought of as depending in part on the goodness of the numerical three-dimensional flow prediction and in part on the physical model accounting for moisture changes and the precipitation process.

We have seen that the precipitation calculations were not too sensitive to the failings of the flow prediction in the two cases studied. To some extent this must be due to the time-wise integrating process (eq. (3)). Since these were only 12-hour predictions, it is difficult to surmise the influence of a continually deteriorating flow prediction over a 24-hour period. On the other hand the predictions of dew point and convective instability, which do not involve such an integration, apparently have not suffered inordinately.

The approximations regarding the condensation process discussed in the Introduction do not appear to be crucial in these cases. A more comprehensive study for a larger number of cases should disclose any systematic effect on the predictions. Relaxation of the constraints introduced by these approximations depends on progress in the field of cloud physics. Without these constraints it should in principle be possible to distinguish between large-scale cloudiness and clear skies.

The approximations which were made only for computational convenience in that portion of the calculations done by hand, may of course be eliminated in programming the entire problem for a high-speed computing machine.

Judging the results of the two cases chosen by the subjective standards normally used for precipitation verification, we conclude a skill comparable to that of the predicted flow.

REFERENCES

1. T. Bergeron, "The Problem of Artificial Control of Rainfall on the Globe, II. The Coastal Orographic Maxima of Precipitation in Autumn and Winter," *Tellus*, vol. 1, No. 3, August 1949, pp. 15–32.
2. B. Bolin and J. G. Charney, "Numerical Tendency Computations from the Barotropic Vorticity Equation," *Tellus*, vol. 3, No. 4, November 1951, pp. 248–257.
3. D. Brunt, *Physical and Dynamical Meteorology*, Cambridge University Press, Cambridge, 1939.
4. J. G. Charney, "Numerical Prediction of Cyclogenesis," *Proceedings of the National Academy of Sciences*, vol. 40, No. 2, February 1954, pp. 99–110.
5. J. G. Charney and A. Eliassen, "A Numerical Method for Predicting the Perturbations of the Middle Latitude Westerlies," *Tellus*, vol. 1, No. 2, May 1949, pp. 38–54.

6. J. G. Charney, R. Fjørtoft, and J. von Neumann, "Numerical Integration of the Barotropic Vorticity Equation," *Tellus*, vol. 2, No. 4, November 1950, pp. 237–254.
7. J. G. Charney and N. A. Phillips, "Numerical Integration of the Quasi-Geostrophic Equations, for Barotropic and Simple Baroclinic Flows," *Journal of Meteorology*, vol. 10, No. 2, April 1953, pp. 71–99.
8. J. R. Fulks, "Rate of Precipitation from Adiabatically Ascending Air," *Monthly Weather Review*, vol. 63, No. 10, October 1935, pp. 291–294.
9. W. F. Libby, Address to American Chemical Society, September 12, 1954.
10. J. S. Sawyer, "A Study of the Rainfall of Two Synoptic Situations," *Quarterly Journal of the Royal Meteorological Society*, vol. 78, No. 336, April 1952, pp. 231–246.
11. J. Smagorinsky, "The Dynamical Influence of Large-Scale Heat Sources and Sinks on the Quasi-Stationary Mean Motions of the Atmosphere," *Quarterly Journal of the Royal Meteorological Society*, vol. 79, No. 341, July 1953, pp. 342–366.
12. R. J. List (Editor), *Smithsonian Meteorological Tables*, 6th Revised Edition, Smithsonian Institution, Washington, D. C., p. 485.
13. M. Tepper, "The Application of the Hydraulic Analogy to Certain Atmospheric Flow Problems," *Weather Bureau Research Paper*, No. 35, October 1952, 50 pp.
14. J. C. Thompson and G. O. Collins, "A Generalized Study of Precipitation Forecasting. Part 1: Computation of Precipitation from the Fields of Moisture and Wind," *Monthly Weather Review*, vol. 81, No. 4, April 1953, pp. 91–100.
15. U. S. Weather Bureau, *Climatological Data for the United States by Sections*, vol. XXXVII, No. 11, November 1950.